Physica Medica 112 (2023) 102627

Contents lists available at ScienceDirect

Physica Medica

journal homepage: www.elsevier.com/locate/ejmp

Organ dose in CT: Comparison between measurements and computational methods

Martina Pace [a], Elisa Bonanno [a], Giuseppina Rita Borzì [a], Nina Cavalli [a], Alessia D'Anna [b], Anna Maria Gueli [b], Giuseppe Stella [b,*], Lucia Zirone [a,b], Camelo Marino [a]

[a] Medical Physics Department, Humanitas Istituto Clinico Catanese, Misterbianco, CT, Italy
[b] Department of Physics and Astronomy E. Majorana, University of Catania, Catania, Italy

ARTICLE INFO

Keywords:
DoseWatch™
EBT-3
XR-QA2
Patient dosimetry
Diagnostic radiology

ABSTRACT

Purpose: This study aims to compare two methods for the organ dose evaluation in computed tomography (CT) in the head- and thorax regions: an experimental method, using radiochromic films, and a computational one, using a commercial software.

Methods: Gafchromic® XR-QA2 and EBT-3 were characterized in terms of energetic, angular, and irradiation configurations dependence. Two free-in-air irradiation calibration configurations were employed using a CT scanner: with the sensitive surface of the film orthogonal (OC) and parallel (PC) to the beam axis. Different dose–response curves were obtained by varying the irradiation configurations and the beam quality (BQ). Subsequently, films were irradiated within an anthropomorphic phantom using CT-thorax and -head protocols, and the organ dose values obtained were compared with those provided by the commercial software.

Results: At different configurations, an unchanged dose response was achieved with EBT-3, while a dose response of 15% was obtained with XR-QA2. By varying BQ, XR-QA2 showed a different response below 10%, while EBT-3 showed a variation below 5% for dose values >20 mGy. For films irradiation angle equal to 90°, the normalized to 0° relative response was 41% for the XR-QA2 model and 83% for the EBT-3 one. Organ dose values obtained with EBT-3 for both configurations and with XR-QA2 for OC were in agreement with the DW values, showing percentage discrepancies of less than 25%.

Conclusions: The obtained results showed the potential of EBT-3 in CT patient dosimetry since the lower angular dependence, compared to XR-QA2, compensates for low sensitivity in the diagnostic dose range.

1. Introduction

At present, computed tomography (CT) dosimetry is predominantly reliant on two metrics, namely computed tomography dose index (CTDI) and dose length product (DLP). These parameters can be conveniently measured using a 100-mm-long ionization chamber and a standard PMMA phantom [1]. However, these indices have several limitations because they could underestimate or overestimate the dose produced by modern CT scanners [2,3].

Organ dose is strongly dependent on the patient effective size. However, this factor is not included in CTDI and DLP measurements, which are primarily utilized for quality assurance and diagnostic reference level verification purposes. As such, these metrics cannot accurately reflect the actual organ dose received by the patient.

The parameter size-specific dose estimate (SSDE) was introduced from the AAPM [4] with the aim of estimating the organ dose from the CTDI multiplied by a correction factor based on the patient effective diameter [4,5]. However, this correction factor can be influenced by uncertainties in CTDI measurements. The AAPM TG 220 [6] asserts that, in the SSDE calculation, the geometric size is used as a surrogate for the patient's X-ray attenuation. Furthermore, the AAPM TG 220 introduces the water equivalent diameter parameter, that provides the patient dimension, using the CT images to obtain the patient attenuation [6]. Dose monitoring systems (DMS) have been developed and deployed globally in recent years to streamline the collection and processing of radiation dose data, facilitate statistical comparisons, enable reporting, and manage radiation dose information [7].

More accurate methods for estimating organ dose in CT are based on either experimental measurements or computational techniques such as Monte Carlo (MC) simulations.

* Corresponding author.
E-mail address: giuseppe.stella@dfa.unict.it (G. Stella).

https://doi.org/10.1016/j.ejmp.2023.102627
Received 29 April 2022; Received in revised form 12 June 2023; Accepted 13 June 2023
Available online 20 June 2023

Many experimental approaches use thermoluminescence dosimeters (TLDs) in combination with an anthropomorphic phantom [8,9].

Giansante et al. performed a study regarding the organ dose in the thorax area: specifically, they compared the organs dose measured by TLDs 100 with that estimated by MC simulations using National Cancer Institute dosimetry system for CT [9]. Giansante et al. conducted dose measurements using anthropomorphic phantoms of both pediatric and adult sizes, and assessed various chest protocols, including "standard," "low dose," and "ultra-low dose." They also investigated the impact of tube current modulation on dose reduction. Results showed that tube current modulation and the type of protocol used could result in up to 35% and 90% dose reduction, respectively, when compared with the standard adult protocol that uses fixed mAs. Moreover, the percent differences found between experimental and MC simulations were within a 20% range.

Other authors have placed both TLDs and radiochromic films between the slabs of anthropomorphic phantom in order to obtain complementary information [10,11].

Radiochromic films can be used in CT applications to obtain bi-dimensional dose distributions when inserted inside an anthropomorphic phantom [11–12]. In this clinical setup, the film sensitive area is not orthogonal to the axis of the CT beam; this results in the introduction of uncertainties due to the angular dependence. Rampado et al. [13] showed that the XR-QA2 response depends on film surface relative position, with respect to the beam axis; specifically, the authors investigated the dose response differences with X-ray beam axis orthogonal to the film surface (0°) and for angles ranging from 0° to 180°. They found that the dose response at 90° was ~50% of the dose response at 0°; the authors have estimated a relative response decrease of 2% integrating over the 0°–360° range.

Several works were published about the characterization of XR-QA2 films and their usage for dosimetric purpose. Tomic et al. [14] studied the energy dependence showing that film response may vary by ±5% with the BQ. The authors demonstrated that it is possible to commit an error of ±14% in the conversion from net reflectance change (ΔR_{net}) to dose if only one calibration curve is used; it is therefore necessary to produce different calibration curves as a function of the BQ.

During the last years high-resolution planar dose distributions were obtained using XR-QA2 model, in combination with an anthropomorphic phantom, to perform 2-D dosimetry in CT [11–12]. Furthermore, it has been shown that 3-D dosimetry could be employed to obtain volumetric reconstruction of dose distribution which can be used to extract information about the irradiated organs [15].

Other works investigated EBT-3 energy response in the typical range of radiodiagnostic applications. Film response was studied after a process of in-air irradiation in the 0.5–4 Gy dose range [16] and in the 0.05–15 Gy one [17]. It has been shown that EBT-3 energy dependence is relatively small for monoenergetic and polyenergetic kV X-ray beams [16], and that it may depend on the absorbed dose [17].

Gafchromic® XR-QA2 model is typically used for radiodiagnostic applications but, due to its stratigraphic composition, it is affected by angular dependence [13,18]; instead, due to its symmetric composition, it can be assumed that the EBT-3 model is less affected by angular dependence [19].

Experimental methods are often laborious and costly. Therefore, many researchers have developed computational approaches for estimating organ dose in CT. Several of these approaches rely on Monte Carlo (MC) methods and implement user-friendly dose calculation tools [20]. These methods are commonly employed in computational simulation of phantoms, CT-scanner models, creation of organ-dose databases, development of effective dose calculation algorithms, modelling of tube current modulation [20–22] and the three-dimensional dose distribution within phantoms [23].

Tian et al. proposed an algorithm [21] based on a library of computational phantoms and simulations of tube current modulation functions chosen based on patient characteristics. This algorithm is the base of the commercial GE DoseWatch™ (DW) software [24], which accurately calculates the dose delivered to various organs during CT examinations. The aim of this study is to compare the experimental and computational methods. The experimental method utilized Gafchromic® films and the Alderson Rando anthropomorphic phantom, while the computational method relied on the DW software to estimate dose values to the organs. Experimental measurements were divided into two steps: the first one consists of the irradiation configuration dependence and the energy and angular characterization of the XR-QA2 and EBT-3 Gafchromic® film; the second one involves the experimental estimation of the dose to the organs using the Gafchromic® films and the comparison between the experimental dose values and those obtained with DW.

2. Materials and methods

2.1. Dose measurement equipment

The XR-QA2 model, typically used for radiodiagnostic applications, is sensitive to a dose range from 0.01 to 20 cGy and an energy range of 20 to 200 kVp (Ashland Advanced Materials, Bridgewater NJ). A 25 μm thick radiation sensitive layer is attached to the 97 μm thick white polyester via a 3 μm thick surface layer. On top of the sensitive layer there is a 15 μm thick pressure-sensitive adhesive to which a 97 μm protective yellow polyester is over-coated.

Gafchromic® EBT-3 is sensitive to a dose range of 0.01 to 30 Gy, and in an energy range of 100 keV to 18 MeV can have a response change of less than 5%. This film consists of an active layer, nominally 28 μm thick, sandwiched between two 125 μm matte-polyester substrates. The active layer contains the sensitive component, a marker dye, stabilizers, and other components giving the film its near energy independent response (Ashland Advanced Materials, Bridgewater NJ).

DW software is a dose management program that offers an organ dose estimation module for CT and is based on a licensed dosimetry technology developed by Duke University [20]. The algorithm used is known as the *Duke University method* and is reported in the literature by Tian et al [21]. According to this method, the dose to the organ is determined by two factors: the patient's anatomy and the resulting dose distribution. Tian et al developed a technique that utilizes a comprehensive library of computational phantoms representing diverse age, size, and sex categories, alongside a range of simulated tube current modulation profiles. Sixty CT images of adult patients were retrospectively selected from the Duke University database. This selection encompasses individuals aged 18 to 78 years with weights ranging from 57 to 180 kg, and the most radiosensitive organs defined by ICRP Publication 103 [25]. The computational phantom library was based on CT-images and was simulated using the model described by Segars et al. who developed the 4D extended cardiac-torso (XCAT) phantom for multimodality imaging research [26,27]. In the Duke University method, the matching between phantom and patient was done in terms of the height of the patient's trunk, as was further explored in the study by Whalen et al [28]. The computational phantoms were combined with a MC simulation to estimate the dose to organs under conditions of constant tube current and modulated tube current.

2.2. Irradiation set up

The irradiations were performed with a GE Revolution Evo CT-scanner operating in the radiodiagnostic department of Humanitas Istituto Clinico Catanese (HICC).

To reproduce the beam qualities used for the head and chest regions at 120 kVp, irradiations were performed using HVL values of 7.6 mm Al and 8.1 mm Al, respectively, and a beam collimation of 64 mm × 0.625 mm. Two irradiation configurations were used (Fig. 1). The orthogonal configuration (OC) was performed with the X-ray tube set at 0° and with the sensitive film surface orthogonal to the beam axis. The parallel

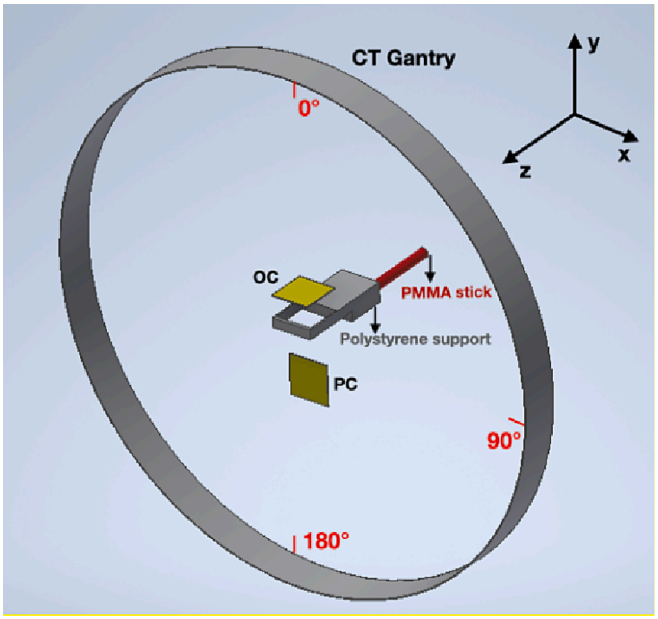

Fig. 1. Irradiation configurations of Gafchromic® films. A PMMA holder was applied to the QA CT phantom holder. A polystyrene support was attached to the end of the PMMA holder to allow for film placement. Orthogonal and parallel configuration are denoted by OC and PC, respectively.

configuration (PC) was performed with the X-ray tube rotating from 0° to 360° and with the sensitive film surface parallel to the beam axis. While the OC reproduces the traditional calibration method for CT applications [11–13,29,30], the PC recreates the positioning of the film when it is located between the slabs of an anthropomorphic phantom undergoing a CT scan.

For each irradiation configuration and BQ, the CT output (mGy/mAs) in air was derived using the CT Dose Profiler (RTI) positioned with the sensor at the CT isocenter.

2.2.1. Energy and angular dependence study

The energy dependence was studied in the dose range from 2 to 65 mGy, by varying the irradiation configuration, HVL and Gafchromic® model. Three film samples were irradiated for each dose value.

The angular dependence study was performed by irradiating the XR-QA2 and EBT-3 films at different angular positions of the X-ray tube: the film samples were placed in air at the isocentre using the OC configuration, and the tube angle was varied from 0° to 180°. Irradiation parameters were set as follows: HVL = 7.6 mm Al, 120 kVp, 160 mAs, and beam collimation of 64 mm and 0.625 mm.

2.2.2. Alderson Rando setup

For organ dose estimation, the anthropomorphic Alderson Rando phantom, shown in Fig. 2, was used.

It is divided axially into 2.5 cm-thick slabs in the cranial-caudal direction. For the head region, slabs 1 to 10 were chosen, and slabs 11 to 20 were selected for the thorax region.

Phantom irradiations were conducted using the CT scanner that was utilized during the characterization phase. The imaging protocols that are most frequently employed for head and thorax examinations in the HICC radiodiagnostic were chosen for these irradiations. The head protocol utilized a consistent mA value of 350 mA, whereas the chest protocol utilized automatic exposure control (AEC). Both CT protocols incorporated helical scanning and a 120 kV setting, and the scan length, as well as the start and end points, were kept constant for each respective region. Scan parameters are given in Table 1. CT scans of thorax and head were performed at two different times and using the two Gafchromic® model. Film samples were placed between the phantom slabs

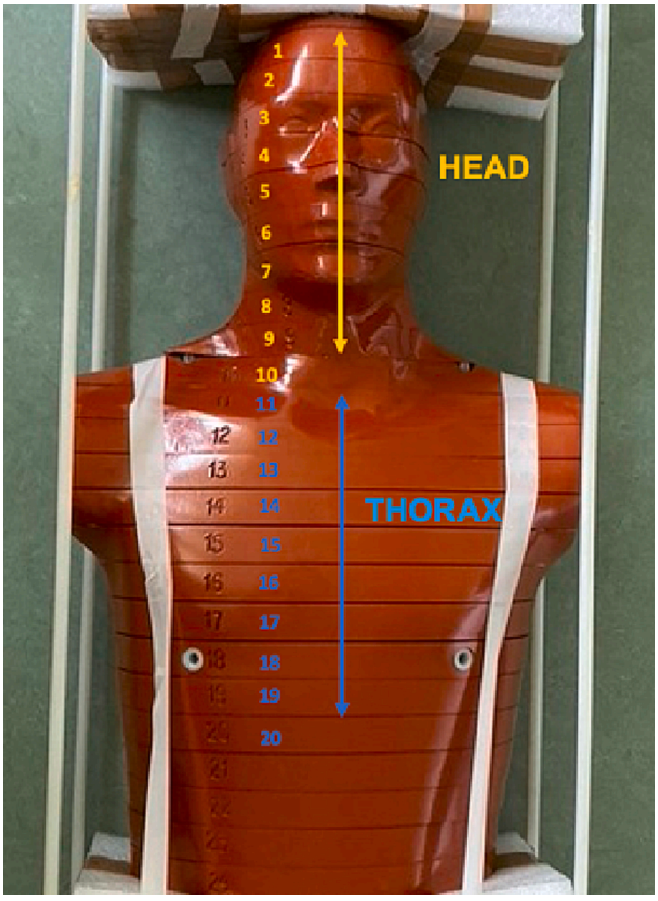

Fig. 2. Alderson Rando anthropomorphic phantom. Slabs 1 to 10 were identified for the scanning region of the head protocol; slabs 11 to 20 were identified for the scanning region of the thorax protocol.

as shown in Fig. 3, following the condition in Table 2. The organs of interest were brain, lungs (left and right), and heart.

2.3. Analysis

2.3.1. Film analysis

The dose response of the XR-QA2 films was evaluated in terms of the net reflectance change (ΔR_{net}), according to equation (1) [29]:

$$\Delta R_{net} = R_{bkg} - R_{irr} = \frac{PV_{bkg} - PV_{irr}}{2^{16}} \quad (1)$$

where R_{bkg} and R_{irr} are the films reflectance before (*bkg* means "background") and after the irradiation (*irr*), PV_{bkg} and PV_{irr} are the pixel values of the films before and after the irradiation, while the term 2^{16} represents the maximum value that can assume a PV in a 16-bit image. The corresponding uncertainty was calculated using equation (2):

$$\sigma_{\Delta R_{net}} = \frac{1}{2^{16}} \sqrt{\left(\sigma_{PV_{bkg}}\right)^2 + \left(\sigma_{PV_{irr}}\right)^2} \quad (2)$$

where $\sigma_{PV_{bkg}}$ and $\sigma_{PV_{irr}}$ are the estimated standard deviation before and after the irradiation, respectively, among the three film samples; $\sigma_{PV_{bkg}}$ and $\sigma_{PV_{irr}}$ included the uncertainties due to the scanner response.

For the EBT-3 the dose response was evaluated in terms of net optical density (OD_{net}), according to equation (3) [29]:

$$OD_{net} = OD_{irr} - OD_{bkg} = log_{10}\frac{PV_{bkg}}{PV_{irr}} \quad (3)$$

where OD is the film optical density, and it is related to its transmittance

Table 1
Technical characteristics of head and thorax protocol used for alderson rando phantom irradiations.

CT Protocol	kV	mA	Rotation time (s)	Pitch (mm)	Collimation (mm)	Irradiation length (mm)	CTDI (mGy)	DLP (mGy*cm)	AEC
Head	120	350	0.4	0.53	32 × 0.625	319.92	47.48	1518.90	No
Thorax	120	320 (mA_{max})	0.4	0.98	64 × 0.625	390.69	4.48	175.20	Yes

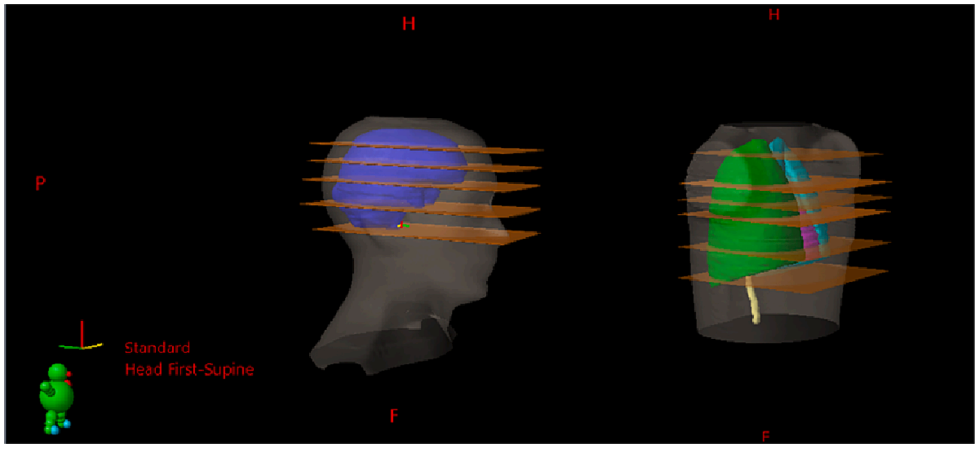

Fig. 3. Contouring, through treatment planning system (TPS) software, of radiochromic films (in orange) between Alderson Rando phantom slice (grey). (For interpretation of the references to color in this figure legend, the reader is referred to the web version of this article.)

Table 2
For each protocol, the number of films used, their size, and the number of the slice on which they were placed are indicated. In the last column, the organs of interest for which the dose was estimated are indicated.

CT Protocol	N° films	Sheets dimension	N° slabs	Organs
Head	5	155 × 225 mm^2	1-2-3-4-5	Brain
Thorax	6	whole sheets	12-14-15-16-18-20	Lungs - Heart

(T) through the relation $OD = -log_{10}T = -log_{10}\frac{PV}{2^{16}}$. In particular, OD_{bkg} and OD_{irr} are the optical density before and after the film irradiation. The statistical uncertainties were calculated using equation (4):

$$\sigma_{OD_{net}} = \frac{1}{\ln 10}\sqrt{\left(\frac{\sigma_{PV_{bkg}}}{PV_{bkg}}\right)^2 + \left(\frac{\sigma_{PV_{irr}}}{PV_{irr}}\right)^2} \quad (4)$$

where $\sigma_{PV_{bkg}}$ and $\sigma_{PV_{irr}}$ are standard deviations estimated before and after the irradiation; also in this case, the terms $\sigma_{PV_{bkg}}$ and $\sigma_{PV_{irr}}$ included the uncertainties due to the scanner response.

For scanning all film samples before and after irradiation, an Epson Expression 10,000 XL flatbed scanner was utilized, and the scanning protocol, which was in accordance with the literature [19,30,31], is shown in Table 3. The scan orientation and potential polarization effects were also taken into consideration [19,31–36]. No colour correction was used.

Images were acquired and saved in.tiff format, then analysed using ImageJ and DoseLab Pro softwares, for XR-QA2 and EBT-3, respectively.

2.3.2. CT images and organ dose analysis

The American Association of Physicists in Medicine (AAPM) TG-61 [37] formalism was employed to calculate the organ dose. The dose absorbed by a specific tissue type through the following equation [38]:

$$Dose(mGy) = (K_{air}^{film})^{air} N_x \left[\left(\frac{\overline{\mu}_{en}}{\rho}\right)_{air}^{w}\right]_{air} B_w C_w^{tissue} \quad (5)$$

where: $(K_{air}^{film})^{air}$ represents the air kerma obtained from analytical relation between ΔR_{net} and OD_{net} film response and CT dose profiler one; N_x is the air kerma calibration coefficient for a particular beam quality; C_w^{tissue} represents the free-in-air ratio of mass energy-absorption coefficients of biological tissue to water, which is dependent on beam quality as indicated by the half value layer (HVL) measurement; $\left[\left(\frac{\overline{\mu}_{en}}{\rho}\right)_{air}^{w}\right]_{air}$ is the ratio of average mass energy-absorption coefficients for water to air, free in air, to convert air kerma to water kerma as a function of HVL (mm Al); B_w is the backscatter factor that accounts for the effect of scattering owing to the water phantom. In this study, considering an SSD = 10 cm and a field diameter of 20 cm, a B_w value of 1.362 was used [37]. For the tissues that were considered, the backscatter factor ratio relative to water did not differ from unity by more than 1% for the field sizes that are commonly used. Thus, it was deemed acceptable to ignore this factor.

The CT images and dosimetric data were processed through the following steps:

1. Contouring of the phantom body, organs, and films using a treatment planning system (TPS), as shown in Fig. 3.
2. Export of the contoured volumes in PLY (Polygon File Format) format to align the radiochromic films and phantom in the CT coordinates, as illustrated in Fig. 4.

Table 3
For each Gafchromic® model, the scanning protocol and accessories used are indicated.

Gafchromic Model	Document type	Document origin	Film type	Image type	Resolution	Accessories
XR-QA2	Opaque	Scan plan	–	48-bit colour	72 dpi	White panel
EBT-3	Film	–	Positive			Plexiglas panel

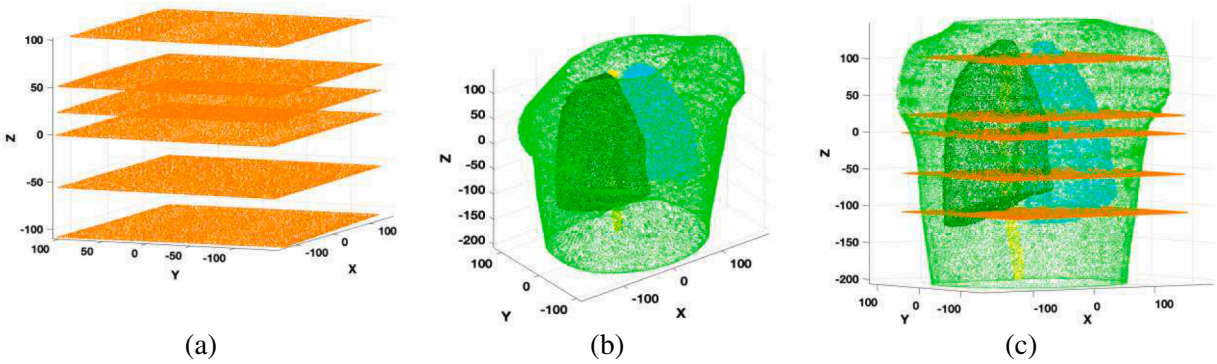

Fig. 4. PLY coordinates of radiochromic film sheets placed in the thorax region (a);.PLY coordinates of the thorax region of Alderson Rando Phantom and his organs (b); overlapping of the.PLY coordinates of the figures (a) and (b).

3. MATLAB script development to:
   - Open the films images in the form of ΔR_{net} and OD_{net} matrix and convert them into dose values matrix (2-D dose maps, Fig. 5) using the appropriate calibration equations.
   - Create a unified three-dimensional spatial reference system in local coordinates for the films and the phantom.
   - Determine the location of each organ on the corresponding film position, as shown in Fig. 5.
   - Extract, for each film, a vector containing the absorbed dose values within the contoured organ and obtain its mean value and standard deviation.

The average absorbed dose value within the contoured organ and its uncertainty were calculated for each film, considering the variability of both the film and scanner response. Next, a weighted mean dose value was obtained for each organ by averaging the mean dose values of the individual films covering the organ.

Finally, an interval in the form $[(D_m - 1\sigma)(D_m + 1\sigma)]$, where D_m is the weighted mean dose value, and $\pm 1\sigma$ within the 95% confidence interval, was obtained. The estimated dose intervals were compared to the confidential intervals provided by the DW software.

3. Results

3.1. Characterization results

In Fig. 6(a) and 6(c) are shown the dose response curves obtained for the XR-QA2 and the EBT-3 models, in terms of ΔR_{net} and OD_{net} versus the absorbed dose in air. Data are divided based on the BQ, and the calibration configurations. The XR-QA2 data were fitted using a rational function ($Dose = \frac{a\Delta R_{net}}{1+b\Delta R_{net}}$), the EBT-3 ones were fitted through a linear function ($Dose = cOD_{net} + d$). The R^2 correlation factors are equal to 0.99 in all cases. In Fig. 6(b) and 6(d) trends of relative uncertainties are shown.

Fig. 7 displays the percentage differences in dose between the films obtained using two irradiation configurations, for the same HVL: $\left|\frac{Dose_{PC} - Dose_{OC}}{Dose_{OC}} \times 100\right|$. In the case of the XR-QA2 model, a relative response above the 15% was found for both the beam qualities throughout the dose range. The EBT-3 model exhibited a decreasing trend as the dose increased, with a relative response of less than 10% observed for doses greater than 20 mGy.

To evaluate the energy dependence of the film, for the same irradiation configuration, the percentage difference in between dose values obtained by varying the two BQs ($\left|\frac{Dose_{HVL=7.6mmAl} - Dose_{HVL=8.1mmAl}}{Dose_{HVL=8.1mmAl}} \times 100\right|$) was evaluated; results are shown in Fig. 8 (a).

The XR-QA2 model demonstrated a response variation of less than

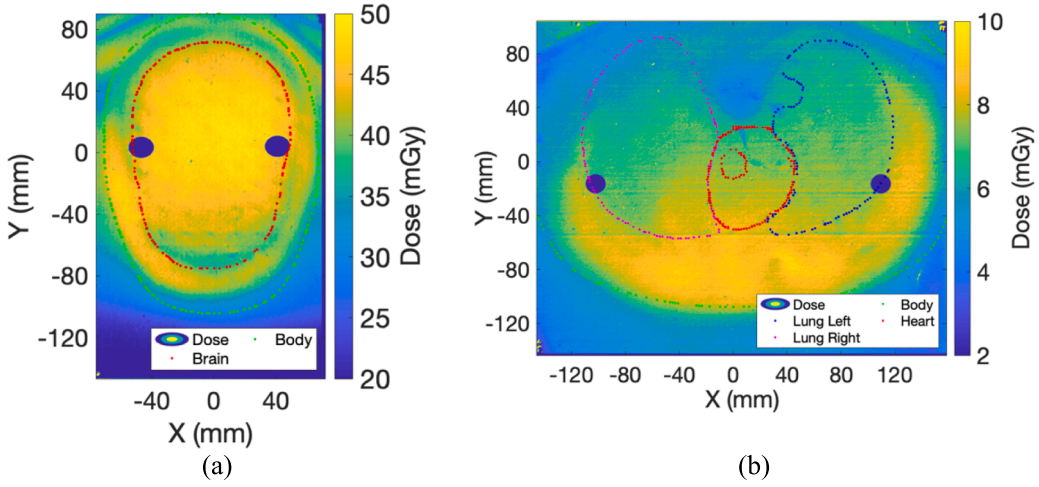

Fig. 5. 2-D false-color dose maps in of the head region (a) and thoracic region (b) in CT coordinates (X and Y), using the XR-QA2 model. Using the.PLY coordinates, the organ contour can be defined: brain (red dots in (a)), lungs (blue and magenta dots in (b)) and heart (red dots in (b)). The green dots represent the body contour. (For interpretation of the references to color in this figure legend, the reader is referred to the web version of this article.)

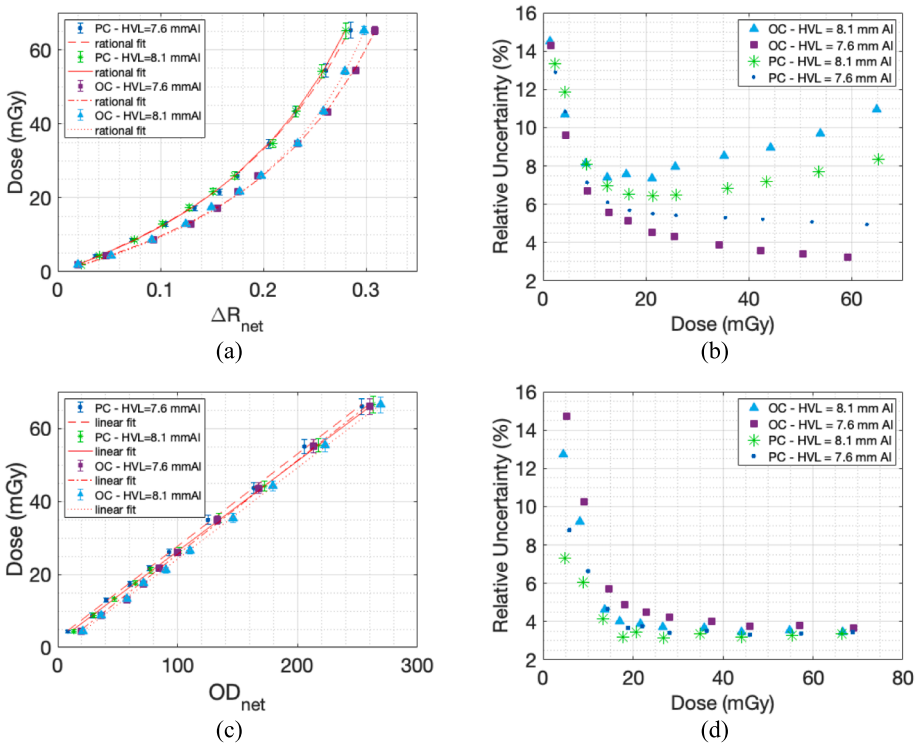

Fig. 6. Dose response curves of Gafchromic® XR-QA2 in terms of ΔR_{net} for the PC and OC, and for the beam qualities: HVL = 7.6 mm Al and HVL = 8.1 mm Al (a), and the relative uncertainties (b). Dose response curves of Gafchromic® EBT-3 in terms of OD_{net} for the PC and OC configuration, and for the bean qualities: HVL = 7.6 mm Al and HVL = 8.1 mm Al (c), and the relative uncertainties (d).

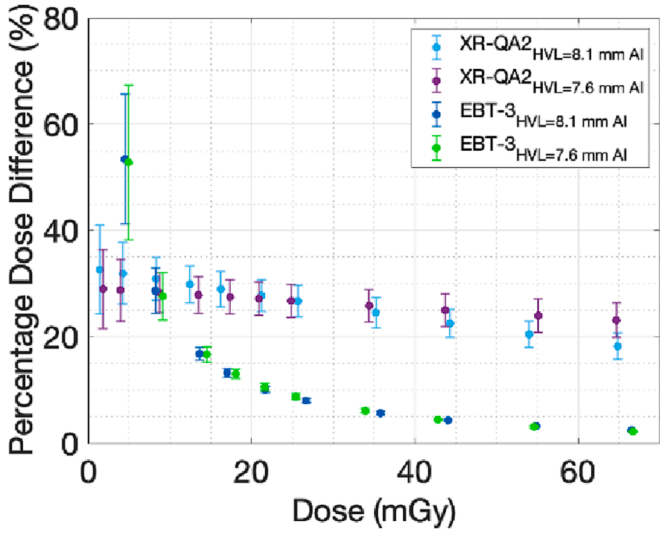

Fig. 7. Percentage dose difference between the two irradiation configurations for XR-QA2 (light blue dots for HVL = 8.1 mm Al, purple dots for HVL = 7.6 mm Al) and EBT-3 (blue dots for HVL = 8.1 mm Al, green dots for HVL = 7.6 mm Al) models. (For interpretation of the references to color in this figure legend, the reader is referred to the web version of this article.)

10% across the entire calibration range, and less than 5% in the range of 4 to 45 mGy. The EBT-3 model exhibited an energy dependence with a decreasing trend: specifically, within the range of 4 to 20 mGy, the response variation was between 18% and 5%, while for dose values above 25 mGy, the response variation was less than 5%. The relative angular dependence is shown in Fig. 8 (b). The data were normalized to the 0° configuration and show a relative dose response around the 100% for the irradiation angle from 0° to 60° and from 120° to 180°. As expected, in the angle range from 80° to 120°, the relative response decreases, and when the irradiation angle is 90°, the relative response is 41% for the XR-QA2 model and 83% for the EBT-3 one.

3.2. Organ dose results

Table 3 shows the dose intervals to organs, in the form $[(D_m - 1\sigma)(D_m + 1\sigma)]$ (see section 2.3.2), estimated using the two film models, and the dose intervals provided by the DW software. Experimental dose intervals per organ were obtained using the organ-specific calibration curve and varying the irradiation configuration (OC and PC). Fig. 9 shows a summary graph illustrating the dose results reported in Table 4.

The XR-QA2 model showed good agreement with the DW for brain and lungs dose, where the OC was used: in these cases, the percentage discrepancies between the experimental and computational methods were around 5% and 13% respectively. However, in the case of brain dose when the PC was used, the discrepancy was less than 20%. Furthermore, the estimated dose intervals for the heart using the OC and the PC, and for the lungs using the PC were outside the range provided by the DW. In fact, the percentage discrepancies between the two methods were about 40%, 83%, and 50% respectively. Otherwise, the dose ranges generated by the EBT-3 model were consistent with those derived from the DW: the percentage discrepancies between the two methods were in all cases lower than 25.5%, and particularly in the case of the brain the discrepancies were less than 6%.

4. Discussion

The results obtained during the characterization show that both film models can be used for CT dosimetry. Since the films response depends on the beam energy, different calibration curves should be used,

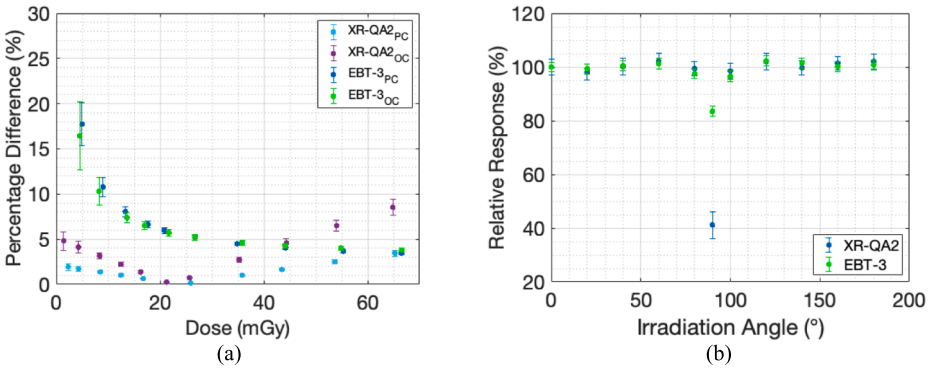

Fig. 8. (a) Percentage difference in dose between the two BQs for XR-QA2 (light blue dots for PC, purple dots for OC) and EBT-3 (blue dots for PC, green dots for OC) models. (b) Relative dose response of XR-QA2 (blue dots) and EBT-3 (green dots) models, at different irradiation angles. (For interpretation of the references to color in this figure legend, the reader is referred to the web version of this article.)

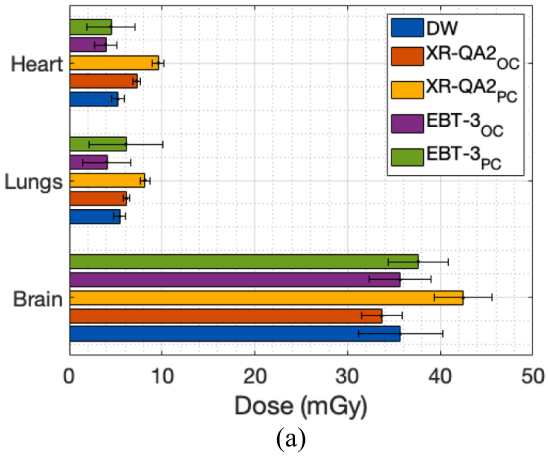

Fig. 9. Dose values provided by DW (blue bar), by Gafchromic XR-QA2 using the OC (orange bar) and using the PC (yellow bar) and by Gafchromic EBT-3 using the OC (purple bar) and using the PC (green bar). (For interpretation of the references to color in this figure legend, the reader is referred to the web version of this article.)

Table 4
Dose intervals obtained for each organ using xr-qa2 and ebt-3 models. D_{m-OC} (D_{m-PC}) is the interval of dose values found using the OC (PC); D_{DW} are the confidence intervals provided by the DW software.

	XR-QA2		**EBT-3**		**DW**
	D_{m-OC}(mGy)	D_{m-PC}(mGy)	D_{m-OC}(mGy)	D_{m-PC}(mGy)	D_{DW}(mGy)
Brain	31.5–35.9	39.3–45.6	32.4–38.9	34.5–40.9	31.1–40.2
Lungs	5.8–6.6	7.6–8.6	1.4–6.7	2.2–10.8	4.8–6.0
Heart	6.9–7.7	9.0–10.2	2.7–5.1	1.9–7.1	4.5–5.9

especially for low dose ranges.

Strong angular dependence was found for the XR-QA2 model in the 90° irradiation configuration, while less angular dependence was found for the EBT-3 model. The observed variations in the film response can be attributed to changes in the irradiation configuration (PC or OC). These results agree with those reported in the literature [13–14], which attribute the lower response of the Gafchromic® XR-QA model to various factors, such as the attenuation of beam as it passes through the film or the fact that only a small fraction of the beam interacts with the film surface.

The XR-QA2 model may not be appropriate for estimating absorbed dose to thoracic organs when utilizing the PC, as it can result in an overestimation of the dose. However, for the head region, the impact of angular dependence appears to be less significant. In fact, the results obtained from both calibration configurations were consistent with those obtained from the DW software.

The results indicate that the EBT-3 model produced dose values that fell within the confidence intervals provided by the DW for all organs and calibration conditions. Additionally, the dose values obtained using the PC configuration were found to be less impacted by angular dependence compared to the XR-QA2 model. This finding is supported by the investigation of film response to different irradiation configurations.

The reason for the difference between the experimental and computational methods could be found not only in the fact that radiochromic films are less sensitive and affected by greater experimental uncertainties at low doses, but also in the limitations of the Duke University model [21]. There are a couple of potential sources of

uncertainty that could impact the accuracy of the results. Firstly, when using AEC in CT examinations, the software employs a current modulation function obtained from MC simulations rather than utilizing the actual current modulation. Secondly, there could be discrepancies between the positioning of the Alderson Rando phantom and the organs inside it compared to the computational phantoms utilized by the DW, which could introduce some level of uncertainty.

According to established standards in CT dosimetry and organ dose estimates, it is generally acceptable for the accuracy of dose values obtained with commercial software to deviate no more than ±20% from the expected value [39,40]. However, when evaluating the results of a study, it is important to note that only the organ dose estimates obtained with the XRQA2 model for the heart using OC and PC, as well as for the lungs using PC, were found to be clinically out of tolerance.

5. Conclusions

Aims of this work were to estimate the organ dose in CT using Gafchromic® XR-QA2 and EBT-3 models, and to compare the experimentally obtained dose values with those provided by the DW software, which is based on the Duke University model [21].

In the initial phase of the study, the radiochromic films were characterized to investigate their energy and angular dependence. The energy dependence analysis revealed the necessity of using different calibration curves depending on the BQ. The analysis of the angular dependence demonstrated a deterioration in film response when the beam axis was parallel to the surface of the films. Additionally, the study on the comparison between the two film models showed that at low doses (thorax region) they respond differently from each other.

The second phase of the study involved estimating organ dose by analyzing dose values slab by slab and varying the film model and irradiation configuration. The resulting dose values were then compared with those obtained from the DW software. The comparison between the two techniques indicated good agreement in the case of dose estimation in the head region, but discrepancies increased in the thorax area, where the doses involved were lower. Nevertheless, both the experimental and computational methods provided a good estimation of the dose to the organs and can give complementary information: while the DW software allowed for immediate dose estimation to individual organs, the use of radiochromic films enabled the acquisition of 2-D and 3-D spatial dose distributions, as well as dose profiles, inside organs in less time.

Declaration of Competing Interest

The authors declare that they have no known competing financial interests or personal relationships that could have appeared to influence the work reported in this paper.

Acknowledgments

The research activity is part of the project APE supported by “Piano di incentivi per la ricerca di Ateneo 2020/2022 (Pia.ce.ri)” – Linea di Intervento 3 – STARTING GRANT of the University of Catania.

References

[1] AAPM The measurement, reporting, and management of radiation dose in CT. Report of AAPM Task Group 23: College Park; MD; 2008.
[2] Damilakis J. CT dosimetry: what has been achieved and what remains to be done. Invest Radiol 2021;56(1):62–8.
[3] Avramova-Cholakova S, Dyakov I, Yordanov H, O'Sullivan J. Comparison of patient effective doses from multiple CT examinations based on different calculation methods. Phys Med 2022;99:73–84.
[4] AAPM Size Specific Dose Estimates (SSDE) in pediatric and adult body CT examinations. Report of the AAPM Tasck Group 204, College Park, MD, 2011.
[5] Sapignoli S, Roggio A, Boschini A, Guida F, Merlo C, Paiusco M, et al. Size-specific dose estimates for pediatric head CT protocols based on the AAPM report TG-293. Phys Med 2022;100:26–30.
[6] McCollough C, Bakalyar DM, Bostani M, Brady S, Boedeker K, Boone JM, et al. Use of water equivalent diameter for calculating patient size and size-specific dose estimates (SSDE) in CT: the report of AAPM Task Group 220. AAPM Rep 2014; 2014:6–23.
[7] Tsalafoutas IA, Hassan Kharita M, Al-Naemi H, Kalra MK. Radiation dose monitoring in computed tomography: status, options and limitations. Phys Med 2020;79:1–15.
[8] Gonzaga NB, Mourão AP, Magalhães MJ, da Silva TA. Organ equivalent doses of patients undergoing chest computed tomography: measurements with TL dosimeters in an anthropomorphic phantom. Appl Radiat Isot 2014;83:242–4.
[9] Giansante L, Martins JC, Nersissian DY, Kiers KC, Kay FU, Sawamura MVY, et al. Organ doses evaluation for chest computed tomography procedures with TL dosimeters: comparison with Monte Carlo simulations. J Appl Clin Med Phys 2019; 20(1):308–20.
[10] Pace M, Stella G, Tonghi LB, Mazzaglia S, Gueli AM. CT-dose measurement of the spinal cord region using XR-QA2 radiochromic films and TLD 100H dosimeters. Instruments 2020;4(3):19.
[11] Brady S, Yoshizumi T, Toncheva G, Frus D. Implementation of radiochromic film dosimetry protocol for volumetric dose assessments to various organs during diagnostic CT procedures. Med Phys 2010;37(9):4782–92.
[12] Boivin J, Tomic N, Fadlallah B, Deblois F, Devic S. Reference dosimetry during diagnostic CT examination using XR-QA radiochromic film model. Med Phys 2011; 38(9):5119–29.
[13] Rampado O, Garelli E, Ropolo R. Computed tomography dose measurements with radiochromic films and a flatbed scanner. Med Phys 2010;37(1):189–96.
[14] Tomic N, Quintero C, Whiting BR, Aldelaijan S, Bekerat H, Liang L, et al. Characterization of calibration curves and energy dependence GafChromic™ XR-QA2 model based radiochromic film dosimetry system. Med Phys 2014;41(6): 062105.
[15] Pace M, Tonghi LB, Mazzaglia S, Stella G, Tuvè C, Gueli A. 3-D dose distribution for organ dose measurement in CT thoracic exams using GafchromicTM XR-QA2 films. J Instrum 2019;14(9):23. P09010.
[16] Eduardo Villarreal-Barajas J, Khan RFH. Energy response of EBT3 radiochromic films: implications for dosimetry in kilovoltage range. J Appl Clin Med Phys 2014; 15(1):331–8.
[17] Massillon-JL G, Muñoz-Molina ID, Díaz-Aguirre P. Optimum absorbed dose versus energy response of gafchromic EBT2 and EBT3 films exposed to 20–160 kV x-rays and 60Co gamma. Biomed Phys Eng Express 2016;2(4):045005.
[18] Giaddui T, Cui Y, Galvin J, Chen W, Yu Y, Xiao Y. Characteristics of Gafchromic XRQA2 films for kV image dose measurement. Med Phys 2012 Feb;39(2):842–50.
[19] Niroomand-Rad A, Chiu-Tsao ST, Grams MP, Lewis DF, Soares CG, Van Battum LJ, Das IJ, Trichter S, Kissick MW, Massillon-Jl G, Alvarez PE, Chan MF. Report of AAPM Task Group 235 radiochromic film dosimetry: an update to TG-55. Med Phys. 2020 Dec;47(12):5986-6025.
[20] Lee C. A review of organ dose calculation tools for patients undergoing computed tomography scans. JRPR 2021;46(4):151–9.
[21] Tian X, Segars WP, Dixon RL, Samei E. Convolution-based estimation of organ dose in tube current modulated CT. Phys Med Biol 2016;61(10):3935–54.
[22] Gandhi D, Crotty DJ, Stevens GM, Schmidt TG. Technical Note: Phantom study to evaluate the dose and image quality effects of a computed tomography organ-based tube current modulation technique. Med Phys 2015;42(11):6572–8.
[23] Costa PR, Nersissian DY, Umisedo NK, Gonzales AHL, Fernández-Varea JM. A comprehensive Monte Carlo study of CT dose metrics proposed by the AAPM Reports 111 and 200. Med Phys 2022;49(1):201–18.
[24] GE Healthcare. DoseWatch: optimized radiation dose management. Available from: https://www.gehealthcare.com/products/dose-management/dosewatch-dose-monitoring-software-ge-healthcare.
[25] Protection R. ICRP publication 103. Ann ICRP 2007;37.2.4:2.
[26] Segars WP, Sturgeon G, Mendonca S, Grimes J, Tsui BM. 4D XCAT phantom for multimodality imaging research. Med Phys 2010;37(9):4902–15.
[27] Segars WP, Bond J, Frush J, Hon S, Eckersley C, Williams CH, et al. Population of anatomically variable 4D XCAT adult phantoms for imaging research and optimization. Med Phys 2013;40(4):043701.
[28] Whalen S, Lee C, Williams JL, Bolch WE. Anthropometric approaches and their uncertainties to assigning computational phantoms to individual patients in pediatric dosimetry studies. Phys Med Biol 2008;53(2):453–71.
[29] Devic S, Tomic N, Lewis D. Reference radiochromic film dosimetry: Review of technical aspects. Phys Med 2016;32(4):541–56.
[30] Butson MJ, Yu PK, Cheung T, Inwood D. Polarization effects on a high-sensitivity radiochromic film. Phys Med Biol 2003;48(15):N207–11.
[31] Devic S. Radiochromic film dosimetry: past, present, and future. Phys Med 2011;27 (3):122–34.
[32] Ferreira BC, Lopes MC, Capela M. Evaluation of an Epson flatbed scanner to read Gafchromic EBT films for radiation dosimetry. Phys Med Biol 2009;54(4):1073–85.
[33] Alnawaf H, Butson MJ, Cheung T, Yu PK. Scanning orientation and polarization effects for XRQA radiochromic film. Phys Med 2010;26(4):216–9.
[34] Alnawaf H, Yu PKN, Butson M. Comparison of Epson scanner quality for radiochromic film evaluation. J Appl Clin Med Phys 2012;13(5):314–21.
[35] Gueli AM, Cavalli N, De Vincolis R, Raffaele L, Troja SO. Background fog subtraction methods in Gafchromic® dosimetry. Rad Meas 2015;72:44–52.
[36] Troja SO, Egger E, Francescon P, Gueli AM, Kacperek A, Coco M, et al. 2D and 3D dose distribution determination in proton beam radiotherapy with GafChromic film detectors. Technol Health Care 2000;8(2):155–64.
[37] Ma CM, Coffey CW, DeWerd LA, Liu C, Nath R, Seltzer SM, et al. American Association of Physicists in Medicine. AAPM protocol for 40–300 kV x-ray beam dosimetry in radiotherapy and radiobiology. Med Phys 2001;28(6):868–93.

[38] Tanabe R, Araki F. Real-time estimation of surface dose based on incident air kerma in diagnostic radiology. Phys Med 2021;89:176–81.
[39] Andersson J, Pavlicek W, Al-Senan R, Bolch W, Bosmans H, Cody D, … Zanca F. (2019). Estimating Patient Organ Dosewith Computed Tomography: A Review of Present Methodologyand Required DICOM Information: A Joint Report ofAAPM Task Group 246 and the European Federationof Organizations for Medical Physics (EFOMP).
[40] Handbook of Basic Quality Control Tests for Diagnostic Radiology IAEA HUMAN HEALTH SERIES N0. 47. Printed by the IAEA in Austria February 2023 STI/PUB/2021.